

# Recent developments in the theoretical study of phase separation in manganites and underdoped cuprates

Elbio Dagotto<sup>1,2</sup>, Seiji Yunoki<sup>1,2</sup>, Cengiz Şen<sup>3</sup>,  
Gonzalo Alvarez<sup>4</sup> and Adriana Moreo<sup>1,2</sup>

<sup>1</sup> Department of Physics and Astronomy, The University of Tennessee, Knoxville, TN 37996, USA

<sup>2</sup> Materials Science and Technology Division, Oak Ridge National Laboratory, Oak Ridge, TN 32831, USA

<sup>3</sup> National High Magnetic Field Laboratory and Department of Physics, Florida State University, Tallahassee, FL 32310, USA

<sup>4</sup> Computer Science and Mathematics Division and Center for Nanophase Materials Sciences, Oak Ridge National Laboratory, Oak Ridge, TN 37831, USA

E-mail: [edagotto@utk.edu](mailto:edagotto@utk.edu)

Received 7 July 2008

Published 9 October 2008

Online at [stacks.iop.org/JPhysCM/20/434224](http://stacks.iop.org/JPhysCM/20/434224)

## Abstract

This paper is a brief review of the status of ‘phase separation’ ideas in manganites and cuprates, mainly focused on the recent efforts by the authors. It is argued that in the last year considerable progress has been made in the understanding of manganites, since the famous colossal magnetoresistance peak in the resistivity versus temperature has been numerically observed in unbiased Monte Carlo simulations using realistic models (namely, including double exchange, phonons, and quenched disorder). It is also conjectured that a phenomenology similar to the one found in manganites could be present in the underdoped regime of the cuprates. It is predicted that a state with superconducting patches exists above the critical temperature in the underdoped regime, in agreement with recent scanning tunneling microscopy experiments.

(Some figures in this article are in colour only in the electronic version)

## 1. Introduction

This is a brief and informal review addressing some recent theoretical results gathered in the context of studies of manganites, the materials with colossal magnetoresistance (CMR), and in the area of the high  $T_c$  cuprates as well. The readers should not consider this paper as a self-contained review; they are encouraged to consult the original literature cited here (mainly the work by our group) and the references therein (where the very important vast effort by other groups is properly cited).

The emphasis is on strongly correlated electrons and phase competition. The latter is emerging as one of the dominant topics of investigation in transition-metal oxides, and other related compounds. Many years of research, both experimental and theoretical, have shown that materials where strong correlation effects are dominant tend to have rich phase

diagrams where many phases compete. This often leads to inhomogeneous states at low temperatures, and concomitant nonlinear responses under the appropriate perturbations (such as magnetic fields in the CMR context).

For instance, research in manganites has been dominated by the idea that the CMR effect is caused by the strong competition between the ferromagnetic (FM) metallic state, caused by double exchange, and insulating states, with charge order (CO), orbital order, and antiferromagnetic (AF) order. Theoretical scenarios have been proposed [1, 2], where it has been argued that the FM and CO/AF states are very different, and likely separated by a first-order phase transition in the clean limit [3]. Upon the introduction of quenched disorder, the intermediate region acquires glassy characteristics and a CMR effect is observed, with the concomitant existence of a novel temperature scale  $T^*$  upon cooling (i.e. the temperature below which local order develops). This is illustrated

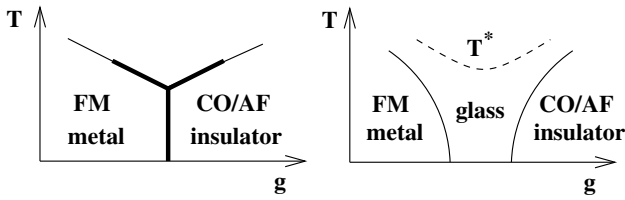


**Figure 1.** Schematic representation of the ideas described in [1–3] for understanding the CMR effect. In the left panel, the proposed phase diagram of manganites in the clean limit is presented. This involves a first-order transition from a FM metal to a CO/AF insulator. In the right panel, the modified phase diagram is shown after the inclusion of disorder. The glassy region above the Curie temperature of the FM metallic phase is the regime where the CMR effect is proposed to occur.

in figure 1. Most of these predictions have been experimentally confirmed [1, 4].

Studies of simple ‘toy models’ [1–3] indeed showed a CMR effect. But the results were obtained using resistor-network approximations, and simplified Hamiltonians [3]. To gain a deeper understanding of the CMR, studies with fundamental models, including double exchange, phonons, and disorder, must be carried out. This is certainly very ‘expensive’ computationally, but fortunately the last year has seen considerable progress in this context (see section 2), and it has now been confirmed that the CMR effect can be observed numerically in realistic models.

The success of theoretical investigations of manganites has implications for research in high  $T_c$  superconductors as well. This transfer of knowledge from one family of materials to the other is regarding the issue of phase competition. The idea is that similarly to the exotic properties of manganites in the CMR regime being caused by the FM versus CO/AF competition, it may occur that the *underdoped* region of the cuprates is dominated by phase competition as well, this time involving AF and superconducting (SC) states. This idea was put forward in [5] and recent experimental results [6] are in excellent agreement with such a proposal, which predicts the presence of superconducting patches above the critical temperature.

This brief communication is organized in a simple manner. First, the most recent results in the CMR context are reviewed. Secondly, a summary of phenomenological results for cuprates is also reviewed. Conclusions are provided at the end. Once again, the short summary presented here is not a full review, and we strongly urge the readers to consult the original literature for further information and to achieve a fair and full view of the tremendous effort by dozens of groups in this fascinating field of research.

## 2. Manganites and the CMR resistivity peak in realistic models

### 2.1. CMR resistivity peak for $J_{AF} = 0$

The most recent computational efforts in the context of theoretical studies of manganites have centered on the search for the CMR peak in the resistivity by using realistic models.

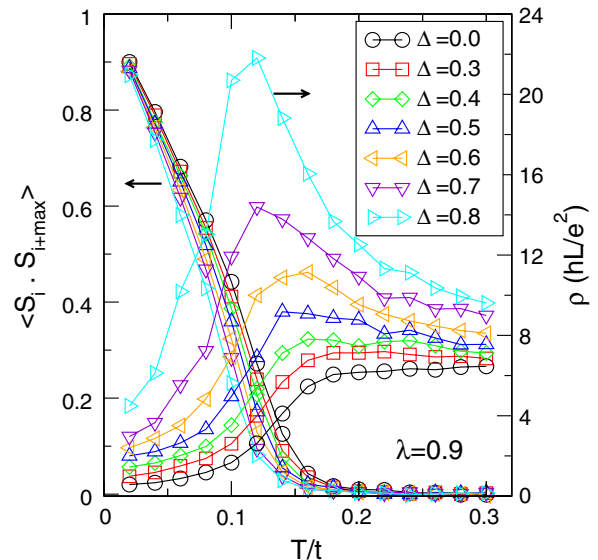


**Figure 2.** Monte Carlo results obtained using a  $4 \times 4 \times 4$  lattice. Shown are the resistivity and spin–spin correlations, the latter at the maximum allowed distance ( $2\sqrt{3}$ ) versus temperature ( $T$ ), working with the one-orbital model at electron–phonon coupling  $\lambda = 0.9$  and electronic density  $n = 0.3$ , and for the disorder strengths  $\Delta$  indicated. The results shown are mainly for one configuration of quenched disorder, but as many as ten configurations were used in particular cases of temperatures and  $\Delta$  s, and no substantial deviations were observed between disorder configurations. These are results reproduced from [7].

As explained in the introduction, a phenomenology of the CMR effect was already envisioned years ago employing simple models and ideas. However, to be fully satisfied with this framework, it is important to achieve the CMR effect using models that are considered ‘realistic’, namely including the double-exchange interaction as well as phonons. Moreover, the study of these models should be done using unbiased techniques. And certainly quenched disorder must be incorporated. Overall, this is a big challenge to our understanding of solids.

The last year has seen tremendous progress in this line of research, and now it can be safely stated that the CMR effect has indeed been observed in calculations that are numerically exact, and whose only input is the Hamiltonian. An example is shown in figure 2, reproduced from [7], where Monte Carlo results using a small lattice are shown. This is for the case of the one-orbital model, in a situation where the FM metallic state competes with a charge-localized insulating state. Results are shown at particular values of the electron–phonon coupling  $\lambda$  and electronic density  $n$  (see the caption), varying the strength of the on-site quenched disorder  $\Delta$ . As the figure indicates, by increasing  $\Delta$  a transition from a metallic state in the clean limit  $\Delta = 0$  to a CMR regime is achieved. The resistivity, calculated with the Landauer formalism, has a clear peak at the location of the Curie temperature. Similar results were also published by another group [8]. In spite of the small system used, a CMR resistivity peak can be observed, which is remarkable.

Moreover, by increasing  $\lambda$  it is possible to get the CMR peak even in the clean limit  $\Delta = 0$ , as figure 3 (left) shows.

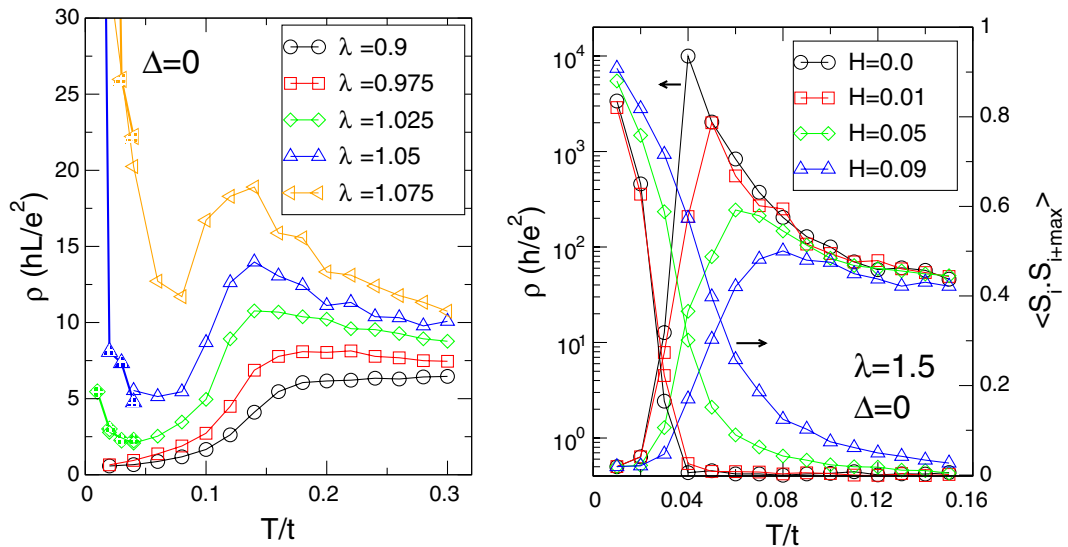


**Figure 3.** Left: influence of the electron–phonon coupling  $\lambda$  in the clean limit  $\Delta = 0$  on the resistivity curve using a  $4 \times 4 \times 4$  lattice at density  $n = 0.3$ . The model used was the one-orbital Hamiltonian with  $J_{AF} = 0$ . Reproduced from [7], where more details can be found. Right: influence of magnetic fields on the resistivity curve and on the spin–spin correlation at the maximum allowed distance ( $4\sqrt{2}$ ) on an  $8 \times 8$  lattice in the clean limit  $\Delta = 0$ , at  $n = 0.1$ . These results are reproduced from [7].

The only price to pay is that the coupling must be fine-tuned to be very close to the metal–insulator transition. This ‘unpleasant’ tuning is avoided by introducing the quenched disorder; thus it is really not a problem.

Applying magnetic fields, the CMR peak found numerically behaves as in experiments. An example is shown in figure 3 (right), obtained at very low density  $n = 0.1$ . The peak is suppressed substantially even for relatively ‘small’ magnetic fields (at least small compared with the natural unit in the problem, the hopping amplitude).

The results in figures 2 and 3 are quite satisfactory, but they still need improvements. To start with, at electronic densities that are not as extreme as  $n = 0.1$ , the CMR peak is not very large and a logarithmic scale is not needed in the figures (see figure 2), contrary to the case for experiments for low bandwidth manganites [1, 2]. More importantly, the experimental phenomenology of manganites indicates that the competitor of the FM metallic state is charge ordered and antiferromagnetic, and this state can be obtained in realistic models for manganites only by including the antiferromagnetic coupling  $J_{AF}$  between the  $t_{2g}$  spins [1, 2]. This improvement will be the focus of section 2.2.

### 2.2. CMR resistivity peak for $J_{AF} \neq 0$

The search for a basic model that contains the famous CMR resistivity peak must necessarily include the coupling  $J_{AF}$  between the localized  $t_{2g}$  spins. The reason is that several years of investigation have shown that this coupling is needed to generate the charge-ordered antiferromagnetic states that are found experimentally, such as the famous CE state near half-doping  $x = 0.5$ . However, including  $J_{AF}$  is not an easy task, since it generates a plethora of states that compete with ferromagnetism, thus causing metastabilities in the Monte Carlo simulations. It is only recently that considerable progress

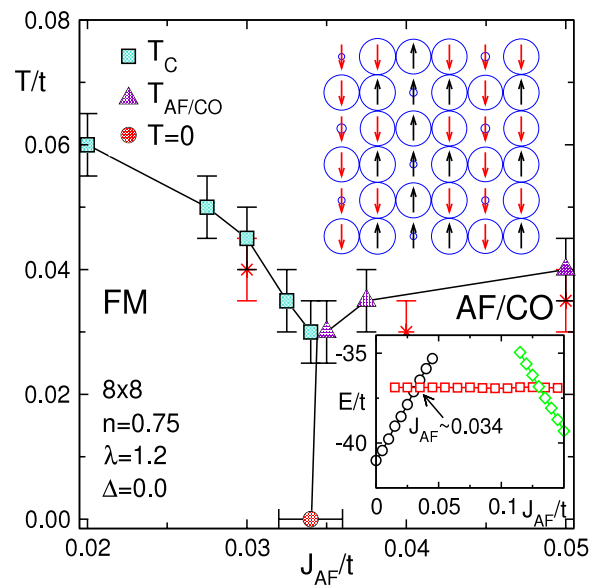


**Figure 4.** Clean limit Monte Carlo phase diagram using  $8 \times 8$  and  $12 \times 12$  lattices, at  $n = 0.75$  and  $\lambda = 1.2$ , reproduced from [9], where more details can be found. The AF/CO state is schematically shown, with the radius of the circles proportional to the electronic density, and arrows representing the  $t_{2g}$  spins. Charge is uniform in the competing FM state. At each temperature,  $10^5$  thermalization and  $5 \times 10^4$  measurement Monte Carlo steps were carried out for the  $8 \times 8$  clusters (and  $\sim 7500$  and  $5000$ , respectively, for the  $12 \times 12$  cluster points indicated by red stars). Inset: energy versus  $J_{AF}$  at very low  $T \sim 0$ , with the FM (CO/AF) phase denoted by black circles (red squares). Green diamonds indicate a G-type AF regime.

has been made, following the extensive use of the XT3 supercomputers at Oak Ridge National Lab. The results were published in [9] and they represent the current state of the art in Monte Carlo simulations.

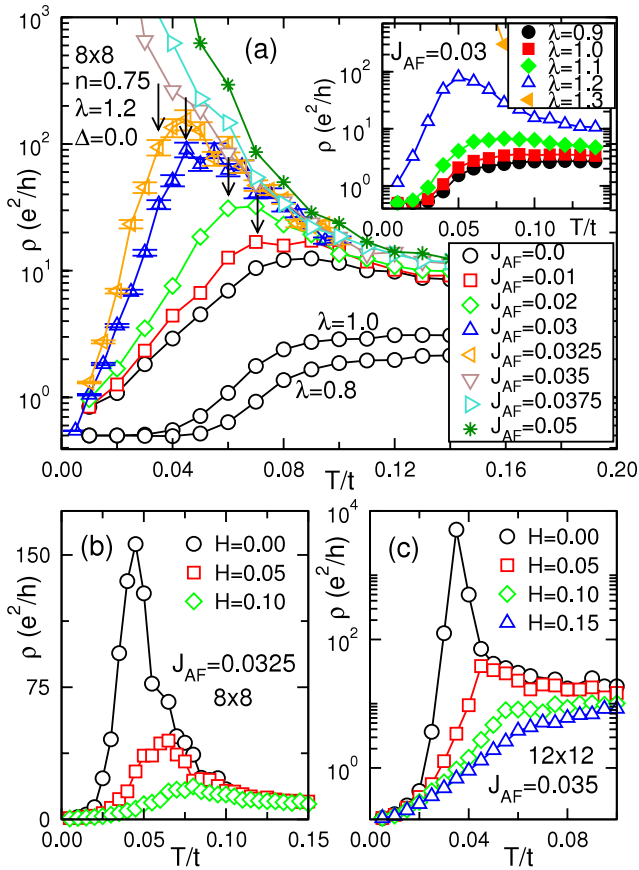


**Figure 5.** Resistivity  $\rho$  versus  $T$  curves for various parameters. (a) Fixing  $\lambda = 1.2$  and varying  $J_{AF}$ . Arrows indicate  $T_C$  s. Results at  $\lambda = 0.8$  and  $\lambda = 1.0$ , with  $J_{AF} = 0.0$ , are also shown. Inset: results fixing  $J_{AF} = 0.03$  and varying  $\lambda$ . (b) Effect of magnetic fields (indicated, in  $t$  units) on  $\rho$  using  $J_{AF} = 0.0325$ , on an  $8 \times 8$  lattice. (c) Same as (b) but for  $J_{AF} = 0.035$ , on a  $12 \times 12$  lattice. These results are reproduced from [9], where more details can be found.

In figure 4, we can observe the phase diagram of the one-orbital model for manganites at density  $n = 0.75$ , which is a realistic electronic density. This phase diagram shows that by varying  $J_{AF}$  it is possible to transition from the FM metallic state to a charge-ordered insulating state with the pattern shown in the figure. This state will be the competitor of ferromagnetism in this analysis. Note that this particular insulating state is *not* claimed to be of experimental relevance *per se*, since it was obtained using only one orbital in the  $e_g$  sector, and for this reason it is not quantitatively realistic. But by studying the one-orbital model with nonzero  $J_{AF}$ , we get one step closer to ‘reality’, as compared with the results in section 2.1. Future work (in progress) is needed to finalize the task by including the two  $e_g$  orbitals in an unbiased simulation.

Perhaps the most outstanding result of recent Monte Carlo simulations is shown in figure 5, which is reproduced from [9]. Here, the resistivity versus temperature is shown to have a peak with a shape and magnitude very similar to those found experimentally in manganites, in the region separating the FM metal from the insulator described in figure 4. Moreover, the addition of magnetic fields reduces the resistivity peak

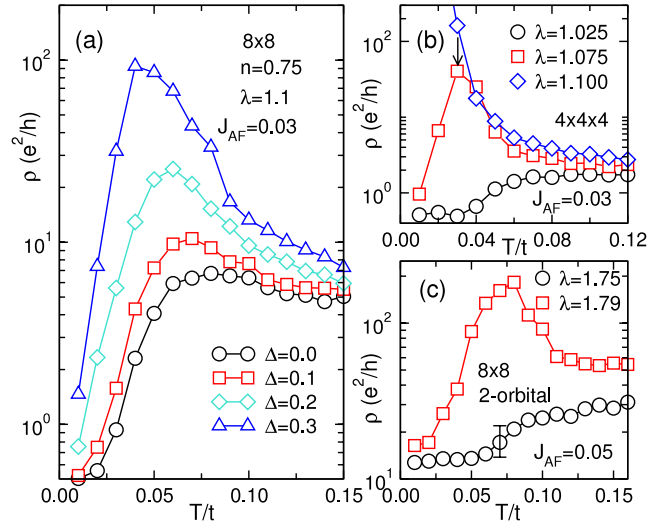


**Figure 6.** Monte Carlo results reproduced from [9], where more details can be found, emphasizing the role of quenched disorder and also including three-dimensional and two-orbital effects. (a)  $\rho$  versus  $T$  in the presence of quenched disorder  $\Delta$ . Up to ten different disorder realizations were used in calculations with quenched disorder. Only small changes between configurations were observed. Monte Carlo steps and starting configurations are as in figure 4. (b)  $\rho$  versus  $T$  using a  $4 \times 4 \times 4$  lattice, parameterized with  $\lambda$ , at  $J_{AF} = 0.03$ . (c) Two orbitals  $\rho$  versus  $T$  results using an  $8 \times 8$  lattice for  $J_{AF} = 0.05$ . In (b) and (c), 4000 thermalization and 4000 measurement Monte Carlo steps were used,  $n = 0.75$ , and the clean limit  $\Delta = 0$  was studied.

drastically, thus causing a genuine large magnetoresistance effect.

As explained before for the case  $J_{AF} = 0$ , the inclusion of quenched disorder removes the need for a careful fine-tuning of couplings, thus increasing the ‘universality’ of the effect. Results in this context can be observed in figure 6, that also includes some results on small three-dimensional lattices, and some preliminary results for two  $e_g$  orbitals as well. For the latter, a vast effort is currently in progress and results will be presented in the near future.

What is causing the CMR effect in the simulations? Clearly, very large length-scale effects, such as micrometer-scale clusters, must be ruled out since the Monte Carlo studies can handle only nanolength-scale clusters. Insight into the origin of the Monte Carlo CMR peaks can be obtained by monitoring the charge–charge correlations as the temperature is decreased in the CMR regime. Results are shown in figure 7, which is reproduced from [9]. There, together with the resistivity versus temperature, there is shown in (a) the charge–charge correlation at distance  $\sqrt{5}$ . Why this peculiar distance? The reason is that  $\sqrt{5}$  and 2 are the two most important hole–hole distances in the charge-ordered arrangement shown in figure 4. The results in (a) show a clear correlation between the resistivity and the  $\sqrt{5}$  charge correlation, as the temperature varies. This indicates that upon cooling in the CMR regime, small regions with the charge arranged in the same way as in the competing state of figure 4 are formed, and they cause the insulating behavior above the Curie temperature. An example is shown in (b), that contains a Monte Carlo ‘snapshot’, namely

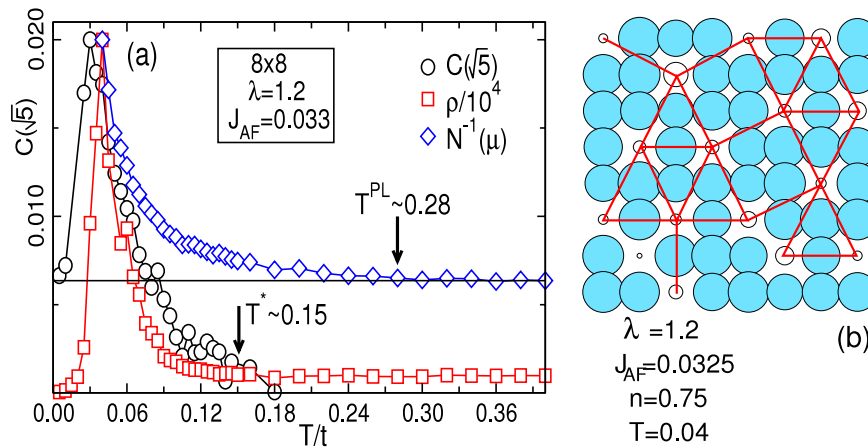


**Figure 7.** (a) Monte Carlo averaged  $C(\sqrt{5})$  (charge–charge correlation at distance  $\sqrt{5}$ ) versus  $T$ , showing a qualitative similarity with the resistivity  $\rho$  (shown). This agreement occurs below the  $T^*$  indicated. At higher  $T$ ,  $\rho$  is flat and  $C(\sqrt{5})$  nearly vanishes. Also shown is the inverse of the density of states  $N(\omega = \mu)$ , to indicate the formation of a pseudogap at  $T^{pl}$ . (b) Typical Monte Carlo snapshot with the radius of the circles proportional to the local charge density. Also shown are the hole–hole distances  $\sqrt{5}$  and 2 of relevance (see the text and [9]).

one of the equilibrium configurations that are of relevance in the CMR insulating regime. The red lines highlight the hole–hole distances that are either  $\sqrt{5}$  or 2. Clearly, those distances are the majority. As the temperature is reduced below the Curie temperature the charge correlation also decreases, and a FM metallic state is formed. Panel (a) of figure 7 also indicates that all the ‘action’ starts at a large temperature  $T^*$ , predicted in studies by Burgy *et al* [3] as the temperature scale where short-range order starts upon cooling. Details can be found in [9].

### 3. Cuprates

The results described in section 2 are very generic, and similar phenomenology should be expected whenever two phases are in strong competition in some particular compound. An example where these concepts can be used is that of the famous high critical temperature Cu oxide superconductors. Here, it is well known that in the phase diagram, particularly in the underdoped regime, there are many competing tendencies, such as antiferromagnetic order, superconductivity, stripes, etc. Then, phenomena similar to those found in manganites could appear in underdoped cuprates as well. This line of investigations was recently pursued by Alvarez *et al* [5]. In their work, a *phenomenological* model Hamiltonian was proposed for the competition between the AF and SC states: it includes noninteracting electrons, that locally interact with classical fields that represent the order parameters, namely a real vector for AF and a complex number for SC. The coupling constant is denoted by  $J$  for AF and  $V$  for SC. Note that this model is *not* of the  $t$ – $J$  or Hubbard variety where superconductivity is supposed to arise from the AF fluctuations, but the model used in [5] is less sophisticated: it simply assumed AF and SC in extreme limits of parameter and, then, the emphasis is on the way AF and SC compete, namely the interesting physics comes from the interpolation. The model can be considered a ‘glorified’ form of the Landau–Ginzburg (LG) approach to phase competition, i.e. ‘integrating

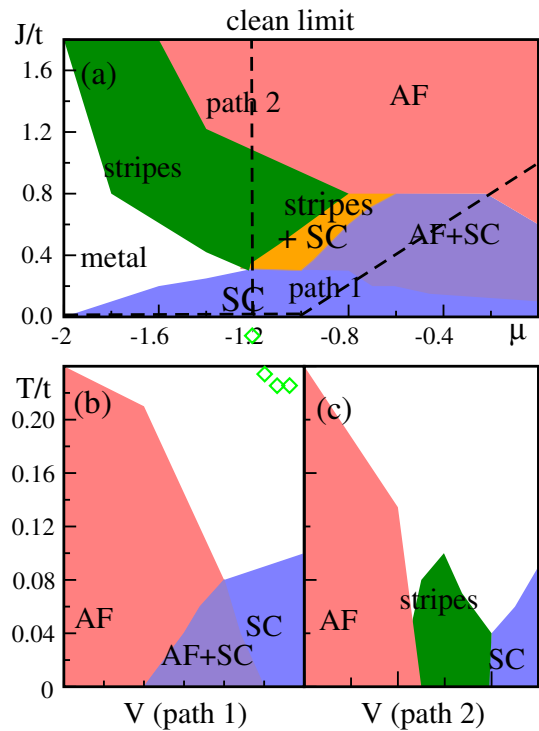


**Figure 8.** (a) Monte Carlo phase diagram for the phenomenological model studied in [5], without disorder at low temperatures. Instead of presenting a three-dimensional phase diagram we have chosen to present a two-dimensional cut along  $V = 1 - J/2$  for simplicity. Five regions are observed: AF, d-wave SC, stripes, coexisting SC + AF, coexisting stripes + SC, and metallic. (b) Monte Carlo phase diagram including temperature along ‘path 1’. (c) Monte Carlo phase diagram along ‘path 2’. This figure is reproduced from [5].

out the fermions’ in the model used in [5]; then LG is expected to be recovered.

The model was studied using Monte Carlo techniques for the order parameters and the exact diagonalization of the electronic sector. Some of the results for the phase diagrams

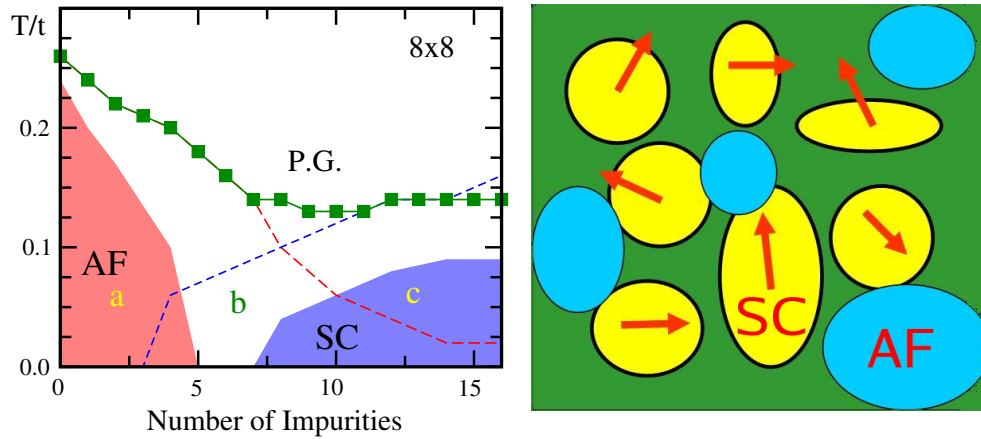


**Figure 9.** Left: phase diagram of the phenomenological model used in [5], after introducing quenched disorder (for details see [5]). The disorder was introduced via plaquette impurities, mimicking Sr doping in single layers.  $\text{Sr}^{2+}$  replaces  $\text{La}^{3+}$ , above the center of a Cu plaquette in the Cu oxide square lattice, donating a hole. Then, as hole carriers are added, a hole-attractive plaquette-centered potential is also incorporated. Near the center of this potential,  $n$  should be sufficiently reduced from 1 that, phenomenologically, tendencies to SC should be expected. With this procedure, the horizontal axis label ‘number of impurities’ is concomitant with ‘hole doping’. The Monte Carlo phase diagram is shown, indicating the presence of a region  $b$  where there is no dominant order, as opposed to the AF in  $a$  and SC in  $c$ . The ‘P.G.’ line denotes the region with a pseudogap in the density of states. Right: schematic representation of the ‘glassy’ state that separates the SC and AF regions, according to the study in [5]. The arrows indicate the phase of the SC order parameter in the many patches. Reproduced from [5].

are reproduced in figure 8. In (a), the zero-temperature phase diagram is shown. The region in between the AF and SC phases is rich, showing that depending on details the interpolation could be via a region of local coexistence of both order parameters (path 1) or a region of stripes (path 2), or (not shown) a first-order transition between the two phases. Including temperature, the phase diagrams in paths 1 and 2 are shown in figures 8(b) and (c). In both cases, an intermediate regime is found, that always has some kind of long-range order. A glassy-disordered state is not observed, contrary to the case for the well-known phase diagram of cuprates such as in  $\text{La}_{2-x}\text{Sr}_x\text{CuO}_4$  ([214]), that has a spin or cluster glass between the AF and SC phases.

To reproduce the [214] results, Alvarez *et al* [5] noticed that the addition of *quenched disorder* was crucial, and the results are in figure 9 (left). Adding disorder creates locally an imbalance between the AF and SC states. This leads to clear dominance of one or the other at the local level, forming clusters, but a concomitant lack of global coherence. In other words, the clusters of AF and SC phases do not communicate well with one another, and there is no global order. In this study, a *pseudogap* (PG) in the density of states is formed, since both phases have gapped states. This PG appears below the original ordering temperature in the clean limit. A crude cartoon of the state found in the phenomenological approach of [5] is shown in figure 9 (right), containing islands of SC and AF phases. The phase of the SC order parameter is random.

The main message of this subsection on cuprates is sketched in figure 10. When a *clean* limit phase diagram is obtained based on a phenomenological model for AF–SC phase competition, phase diagrams (a)–(c) are obtained, namely the transition from AF to SC can occur via local coexistence of the two order parameters, a first-order transition, or even via stripes involving lines of both order parameters. None of these reproduce the real phase diagram

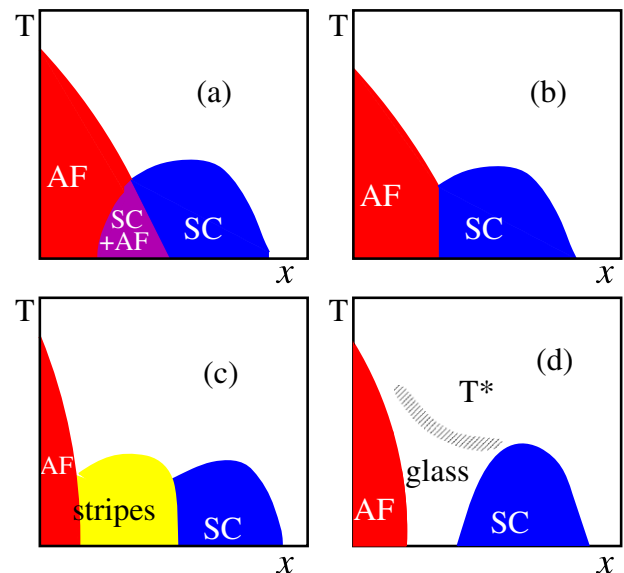


**Figure 10.** Schematic representation of the phase diagrams that the models studied in [5] present, in the clean (a), (b), (c) and dirty (d) limits. In the clean limit, regions with *local* coexistence of AF and SC (panel (a)), or a first-order transition separating AF from SC (panel (b)) with the first-order character of the transition possibly continuing in the AF-disordered and SC-disordered transitions, or an intermediate striped regime (panel (c)) are possible. None of these reproduce the phase diagram of cuprates with an intermediate glassy state. This is achieved only by adding quenched disorder (see panel (d)). In this regime, a  $T^*$  temperature is found below which a pseudogap exists in the density of states. This phase diagram has similarities with those proposed before for manganites [1, 2], and certainly it is in excellent agreement with the experimental phase diagram of LSCO. For more details, see [5].

of  $\text{La}_{2-x}\text{Sr}_x\text{CuO}_4$ . However, on simply adding quenched disorder, the result (d) is obtained, which has a much better agreement with experiments.

Then, as in manganites, the consideration of quenched disorder is important in cuprates. Moreover, it is possible to imagine that the analogy with manganites goes beyond phase diagrams: the glassy state figure 9 (right) may lead to very large (colossal?) responses, the analogue of the CMR effect in manganites. This large responses could take place in the SC sector, by rapid alignment of the phase factors of the SC islands, upon the introduction of an external perturbation, such as the proximity of another SC phase. More details can be found in [5].

#### 4. Summary and discussion

During the last couple of years, a remarkable progress has been achieved in the study of manganites using realistic models. This progress was mainly made possible by building upon the previous phenomenological approaches, that clearly established phase competition as the main source of the CMR effect, and also by using modern supercomputers, such as the XT3 at Oak Ridge National Laboratory. The main result in this context has been the clear observation of a peak in the resistivity versus temperature, that is rapidly suppressed with increasing magnetic fields. The origin of this effect was identified: it is the development of short-range charge order above the Curie temperature, in the CMR regime. This successful scenario for manganites has implications for other transition-metal oxides as well, particularly the cuprates. There was here also reviewed the recent proposal that explains the underdoped regime of the cuprates in terms of an inhomogeneous state involving superconducting patches, with a nonzero amplitude for the superconducting order parameter, but lack of coherence among the phases of the many patches. This is in agreement with very recent experiments [6]. The issue of phase separation in transition-metal oxides is rapidly developing into one of the most important areas of research in strongly correlated materials, and it is anticipated that exotic phenomena may emerge in the parameter regime where this competition occurs.

#### Acknowledgments

This research has been supported mainly by NSF via grants DMR-0443144 and DMR-0706020. This effort has also been sponsored by the Division of Materials Sciences and Engineering of the Department of Energy, USA. Most of the computational work was performed on the Cray XT3 of the National Center for Computational Sciences at Oak Ridge National Laboratory.

#### References

- [1] Dagotto E 2002 *Nanoscale Phase Separation and Colossal Magnetoresistance* (Berlin: Springer)
- [2] Dagotto E, Hotta T and Moreo A 2001 *Phys. Rep.* **344** 1  
Yunoki S, Hu J, Malvezzi A, Moreo A, Furukawa N and Dagotto E 1998 *Phys. Rev. Lett.* **80** 845  
Moreo A, Yunoki S and Dagotto E 1999 *Science* **283** 2034 and references therein
- [3] Burgy J, Mayr M, Martin-Mayor V, Moreo A and Dagotto E 2001 *Phys. Rev. Lett.* **87** 277202  
See also Burgy J, Moreo A and Dagotto E 2004 *Phys. Rev. Lett.* **92** 097202
- [4] Tomioka Y and Tokura Y 2004 *Phys. Rev. B* **70** 014432 and references therein  
See also Akahoshi D, Uchida M, Tomioka Y, Arima T, Matsui Y and Tokura Y 2005 *Phys. Rev. Lett.* **90** 177203
- [5] Alvarez G, Mayr M, Moreo A and Dagotto E 2005 *Phys. Rev. B* **71** 014514  
See also Mayr M, Alvarez G, Moreo A and Dagotto E 2006 *Phys. Rev. B* **73** 014509
- [6] Gomes K K, Pasupathy A N, Pushp A, Ono S, Ando Y and Yazdani A 2007 *Nature* **447** 569 and references therein
- [7] Sen C, Alvarez G, Aliaga H and Dagotto E 2006 *Phys. Rev. B* **73** 224441  
See also Sen C, Alvarez G and Dagotto E 2004 *Phys. Rev. B* **70** 064428
- [8] Kumar S and Majumdar P 2006 *Phys. Rev. Lett.* **96** 016602 and references therein
- [9] Sen C, Alvarez G and Dagotto E 2007 *Phys. Rev. Lett.* **98** 127202